

doi: 10.13241/j.cnki.pmb.2017.26.017

## 鞍旁海绵状血管瘤的 MRI 诊断及误诊分析

吕秀花<sup>1</sup> 蔺新梅<sup>2</sup> 李 陈<sup>1</sup> 王 虹<sup>1</sup> 印 弘<sup>1△</sup>

(1 第四军医大学西京医院放射科 陕西 西安 710032;2 解放军第十医院 甘肃 武威 733000)

**摘要 目的:**分析鞍旁海绵状血管瘤 MR 影像特点及误诊原因,提高对该疾病的诊断及鉴别诊断水平。**方法:**收集我院经手术病理证实的 13 例鞍旁海绵状血管瘤,术前均行 MRI 平扫及增强扫描,5 例行 3D-ASL 检查,分析其影像学资料。**结果:**9 例表现为横向哑铃状,鞍旁大,鞍内小,病灶主体位于颈内动脉外侧,颈内动脉海绵窦段被病灶包绕;1 例鞍旁与鞍内病灶大小相似,1 例病灶主体位于颈内动脉内侧,2 例病灶完全位于颈内动脉外侧;7 例垂体显示不清,6 例垂体受推移;6 例 T2WI 表现为类似脑脊液的极高信号;仅 5 例行 3D-ASL 检查,病灶均呈低灌注。误诊 9 例,其中 4 例误诊垂体腺瘤,5 例误诊脑膜瘤。**结论:**横向哑铃状、病灶主体位于颈内动脉外侧及 T2WI 类似脑脊液的极高信号是鞍旁海绵状血管瘤的典型影像特征。对于不典型病变,借助 3D-ASL 可以减少误诊,充分掌握 MRI 影像特征及鉴别诊断的要点,对提高临床术前诊断水平具有重要价值。

**关键词:**海绵状血管瘤;鞍旁;磁共振成像**中图分类号:**R445.2; R739.4 **文献标识码:**A **文章编号:**1673-6273(2017)26-5083-04

## Analysis of MRI Diagnosis and Misdiagnosis of Parasellar Cavernous Haemangioma

LV Xiu-hua<sup>1</sup>, LIN Xin-mei<sup>2</sup>, LI Chen<sup>1</sup>, WANG Hong<sup>1</sup>, YIN Hong<sup>1△</sup>

(1 Department of Radiology, Xijing Hospital, Fourth Military Medical University, Xi'an, Shaanxi, 710032, China;

(2 Department of Radiology, the Tenth Hospital of PLA, Wuwei, Gansu, 733000, China)

**ABSTRACT Objective:** To analyze the magnetic resonance imaging (MRI) features of parasellar cavernous haemangioma and improve the diagnosis and differential diagnosis accuracy. **Methods:** 13 patients with parasellar cavernous haemangioma were collected. All the patients were diagnosed by MRI and confirmed by pathology. Based on the pathologic findings, the MRI features were discussed. **Results:** 9 cases presented horizontal dumbbell. The lesions located in the parasellar were larger than the sella turcica. The main body position of the lesions were centered lateral to the parasellar and encasesed the intracavernous internal carotid artery (ICICA). While, 1 cases were similar in size and shape. 1 case was located in the sella turcica. 2 cases was centered lateral to the ICICA. pituitary were detected obscurity in 7 cases and displaced in 6 cases, 6 cases appeared extremely high homogeneous intensity on T2-weighted images: as bright as cerebrospinal fluid signal. Only 5 cases underwent three-dimensional arterial spin labelling perfusion imaging (3D-ASL). The lesions revealed marked hypoperfusion. The cases of misdiagnosis were 9, including 4 pituitary adenomas and 5 meningiomas. **Conclusions:** The characteristics of MR images of parasellar cavernous haemangioma were horizontal bottle gourd form, the main body position of the lesions were centered lateral to the parasellar and encasesed the (ICICA), and their extremely high homogeneous intensity on T2-weighted images: as bright as cerebrospinal fluid signal. In cases that are equivocal, 3D-ASL were useful in differentiating cavernous haemangiomas from parasellar meningiomas, which could decrease mistaken diagnosis. Grasping the imaging feature and differential diagnosis were helpful for the diagnosis of this disease.

**Key words:** Cavernous haemangioma; Parasellar; Magnetic resonance imaging**Chinese Library Classification(CLC):** R445.2; R739.4 **Document code:** A**Article ID:** 16736273(2017)26-5083-04

### 前言

鞍旁海绵状血管瘤比较罕见,该肿瘤占鞍旁区所有病变的比例不到 2%,其与鞍旁脑膜瘤、神经鞘瘤等的鉴别诊断较为困难<sup>[1]</sup>,临床误诊率高。该疾病国内外文献报道较少,常以个案形

式报道,鞍旁不同肿瘤的治疗方式不同,海绵状血管瘤若采用手术方式极易导致大出血,海绵状血管瘤放疗效果较好<sup>[2]</sup>。因此,术前能否明确诊断,减少误诊对于临床决策具有重要意义,本研究回顾性分析鞍旁海绵状血管瘤 MR 影像特点,旨在提高对该疾病的诊断及鉴别诊断水平。

### 1 资料与方法

#### 1.1 临床资料

选取本院 2010 年 2 月 -2016 年 6 月间全部术后经病理确诊鞍旁海绵状血管瘤患者 13 例,均采用 MRI 平扫及增强扫描

作者简介:吕秀花(1982-),硕士,主治医师,主要研究方向中枢神经系统、乳腺多模态影像疾病诊断,电话:15891309466,

E-mail: lxhybwz@163.com

△ 通讯作者:印弘,E-mail: yinhong@fmmu.edu.cn

(收稿日期:2016-12-05 接受日期:2016-12-30)

进行术前诊断,5例行三维动脉自旋标记(3D-ASL)检查。患者男5例,女8例,年龄28~56岁,平均46.2±12.2岁;病程3个月~8年,临床表现头痛、头晕2例,眼睑下垂3例,面部麻木3例,视力下降2例,复视1例,月经紊乱1例,体检时偶然发现1例。

## 1.2 检查设备与方法

采用GE Discovery MR750 3.0 T或Siemens Magnetom Trio Tim3.0 T超导型磁共振扫描仪,使用32通道或8通道头颅相控线圈,行横断面T1WI、T2WI,矢状位T1WI平扫,扫描参数设定T1WI:TR1750 ms,TE24 ms;T2WI:TR4252 ms,TE103.7 ms,层厚5 mm,层间距1 mm,经肘正中静脉注射顺磁性对比剂钆喷替酸甲胺(Gd-DTPA,0.1 mmol/kg)以2.0 mL/s静脉注射进行横断、矢状位、冠状位增强扫描扫描;根据临床需求行3D-ASL扫查患者在增强前进行该序列扫描,3D-ASL成像:采用标准连续动脉旋标记成像,参数设定TR=4653 ms,TE=10.5 ms,标记延迟时间1525 ms,层厚4.0 mm,无层间距。

## 2 结果

### 2.1 影像特点

13例海绵窦区病灶,左侧8例,右侧5例;病灶最大横径3.5~7.5 cm。9例呈横向哑铃状,边界清晰,鞍旁病灶大,鞍内小,颈内动脉海绵窦段被病灶包绕,T1WI均可以看到典型的流空征象,病灶主体位于颈内动脉外侧,轴位、冠状位均显示病灶主体位于鞍旁,由鞍旁向鞍内侵犯(图1A、2A);另外1例鞍旁与鞍内病灶大小相似,1例病灶主体位于颈内动脉内侧(图2A-C),2例病灶完全位于颈内动脉外侧。常规MRI平扫T1WI病灶呈等或稍低信号,6例病灶T2WI表现为类似脑脊液的极高信号(图1A),3例呈稍高信号(图2B),4例信号不均;7例病灶平扫及增强病灶与垂体分界不清,鞍内二者边界、信号混淆,6例垂体受推移;增强扫描病灶明显强化,9例强化均匀(图1B),4例强化不均(图2C);仅5例行3D-ASL检查,5例3D-ASL均显示病灶区域呈低灌注(图2D)。

### 2.2 误诊分析

13例病例,9例出现误诊,其中4例误诊为垂体腺瘤,另外5例误诊为脑膜瘤。

4例误诊为垂体腺瘤的主要影像特点:1例病灶主体位于颈内动脉内侧,T2WI呈稍高信号,垂体显示不清,增强扫描呈不均匀强化,内见囊变(图2A-C)。另外3例,病灶主体均位于颈内动脉外侧,T2WI呈稍高信号,颈内动脉海绵窦段均受包绕,垂体均显示不清,其中1例增强扫描呈均匀强化,2例可见囊变,强化不均,4例鞍隔上下均可见病灶。

5例误诊为脑膜瘤的主要影像特点:1例病灶鞍内与鞍外大小相似,T2WI呈稍高信号,见硬膜尾征,增强扫描均匀强化;另外4例,病灶主体均位于颈内动脉外侧。其中1例呈横向哑铃状,T2WI均呈极高信号,病灶局部通过视神经管向肌锥内延伸,增强扫描呈均匀强化(图1A-B),其余3例T2WI均呈极高信号,2例可见脑膜尾征。

## 3 讨论

鞍旁海绵状血管瘤发病率低,临床对该病影像特点认识不

足,容易误诊。文献<sup>[3]</sup>报道其被误诊为脑膜瘤的误诊率高达66.7%~87.5%。此外,侵袭性垂体瘤临床及影像表现与其相似,易于混淆,导致误诊。为了进一步提高该肿瘤的诊断准确率,本文对其MRI影像特点进行回顾性分析,旨在提高诊断及鉴别诊断水平。

颅内海绵状血管瘤分为脑内和脑外两种类型,脑内海绵状血管瘤诊断较为容易,而脑外型主要好发于海绵窦。最近,潘力等<sup>[4]</sup>根据MRI冠状位上肿瘤与颈内动脉垂直线的关系,提出了基于影像学的新分型,其可分为鞍内型、鞍旁型、混合型三种类型,并总结了目前单中心例数最多的海绵窦海绵状血管瘤(53例)伽马刀治疗结果,研究表明伽马刀治疗安全有效,并可能替代传统的外科手术,成为中小型海绵窦海绵状血管瘤的首选治疗方法,因此能否准确诊断尤为重要。

鞍旁海绵状血管瘤病理学特点肉眼下见病灶是由一簇扩张的血管构成,切面呈海绵状,血管壁无肌层和弹力纤维层,仅由菲薄的胶原纤维和内皮细胞所构成,管腔内充满血液,管腔间可相互连通,病理可分为A、B两型,A型由大量薄壁血管组成,伴有单层内皮排列的毛细血管;B型则含有大量实质成分和形成良好的血管结构,其间质成份及弹力纤维多<sup>[5]</sup>,因此,有研究显示MRI平扫A型多表现为均匀常T2信号,而B型则多表现为信号不均<sup>[6]</sup>。MRI增强扫描A型海绵状血管瘤表现为显著均匀强化,B型海绵状血管瘤则表现为不均匀渐进性强化<sup>[7]</sup>,另有研究表示海绵状血管瘤MRI增强扫描在以后的5 min内进行性均匀充盈整个肿瘤<sup>[8]</sup>。

以往对海绵窦海绵状血管瘤的影像分析报道,按照新分型,大多指混合型,鞍内型的报道甚少,文献多为个案报道。2014年,王凯等<sup>[9]</sup>报道总结国外仅5例,国内仅7例,文中提出鞍内海绵状血管瘤术前诊断非常困难,与垂体腺瘤难鉴别。MRI及CT的冠状位仅能提供辅助诊断,本研究回顾性分析的海绵状血管瘤仅1例病灶为鞍内型。鞍旁型和混合型相对鞍内型常见,研究结果显示2例为鞍旁型,病灶位于颈内动脉外侧;10例为混合型,病灶主体位于颈内动脉外侧,颈内动脉海绵窦段包埋其中,病灶呈横向哑铃状,外大内小,1例鞍旁与鞍内病灶大小相似。MRI诊断鞍旁海绵状血管瘤较其它影像检查手段具有高的敏感性和特异性<sup>[10]</sup>,以往文献<sup>[11]</sup>报道鞍旁海绵状血管瘤典型的影像特征为T1WI均为近似脑灰质信号,T2WI表现为脑脊液相似的极高信号,T2WI极高信号的诊断价值较高。本研究9例呈横向哑铃状,边界清晰,鞍旁病灶大,鞍内小,颈内动脉海绵窦段被病灶包绕,T1WI均可以看到典型的流空征象。常规MRI平扫T1WI病灶呈等或稍低信号,6例病灶T2WI表现为类似脑脊液的极高信号,与文献报道基本一致。但2例鞍旁与鞍内病灶大小相似,4例病灶完全位于颈内动脉外侧,6例病灶平扫及增强病灶与垂体分界不清,鞍内二者边界、信号混淆,3例T2WI呈稍高信号,4例信号不均,此不典型特征给诊断带来了困难。

结果显示9例出现误诊,4例误诊为垂体腺瘤,5例误诊为脑膜瘤。本病误诊垂体腺瘤关键原因是对该病变影像特征认识不足,缺乏经验,更多的关注垂体,因正常垂体显示不清,误认为病灶突破鞍隔,向鞍外生长,二者临床症状又极其相似,因此很容易导致误诊。垂体大腺瘤典型影像特点以鞍底向上生长,

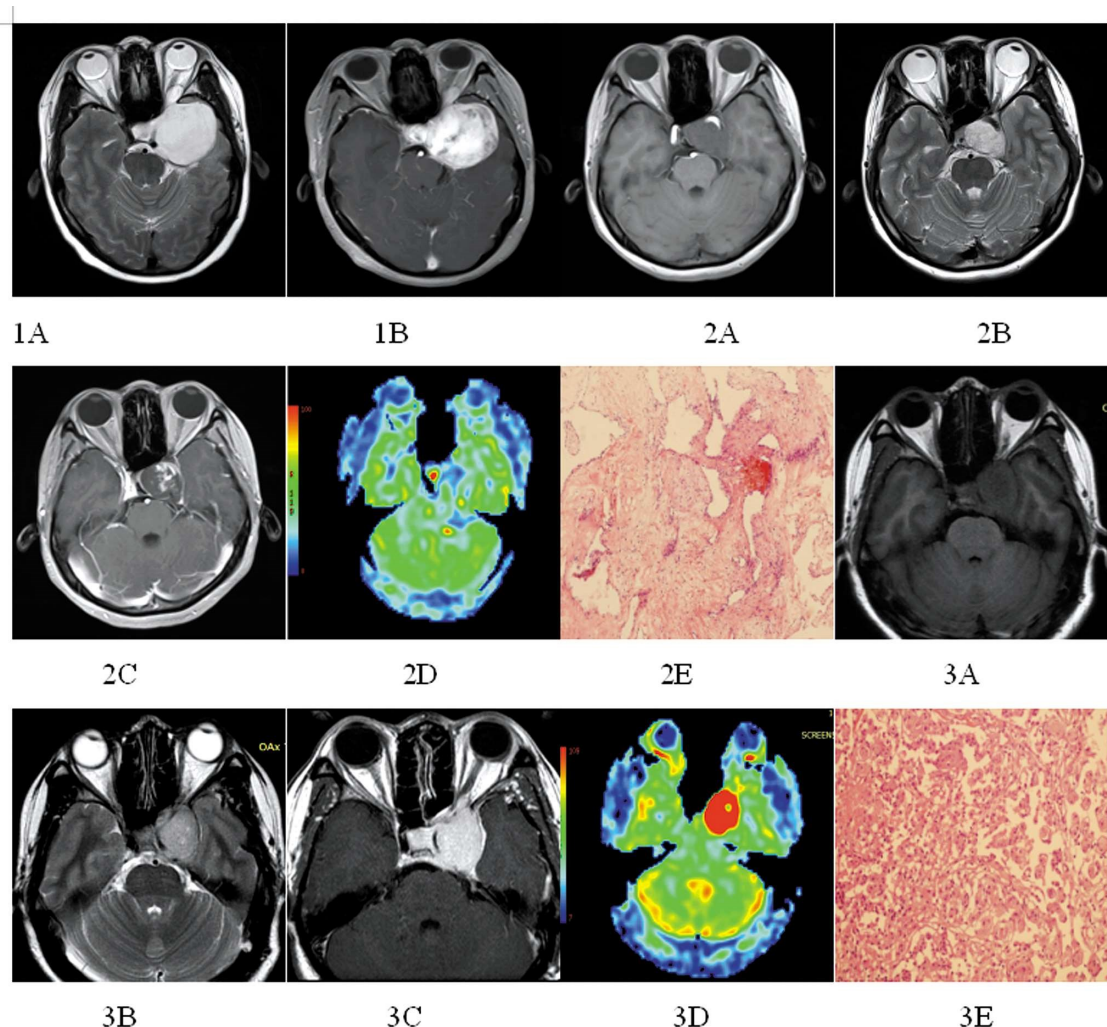


图 1 鞍旁海绵状血管瘤与脑膜瘤

Fig. 1 Parasellar cavernous haemangioma and meningioma

Fig. 1A-B: a 53-year-old woman with a left parasellar cavernous haemangioma. MR images show that the mass produces a homogeneous and markedly high signal intensity on axial T2-weighted images (Fig. 1A) and is strongly homogeneous enhanced on axial postcontrast T1-weighted image (Fig. 1B). The case The lesion located in the parasellar is larger than the sella turcica and was mistaken for meningiomas. Fig. 2A-E: a 56-year-old woman with a left parasellar cavernous haemangioma. MR images show that the mass produces isointensity on axial T1-weighted (Fig. 2A) and a homogeneous and high signal intensity on axial T2-weighted images (Fig. 2B) and is heterogeneous enhanced on axial postcontrast T1-weighted image (Fig. 2C); the mass encircles the left ICA; the mass is located in the sella turcica and was mistaken for pituitary adenomas. 3D-ASL CBF map (Fig. 2D) shows relative hypoperfusion; pathology, HE staining (Fig. 2E) indicated cavernous haemangioma. Fig. 3A-E: a 60-year-old man with a left parasellar cavernous parasellar meningioma. MR images show that the mass produces isointensity on axial T1-weighted (Fig. 3A) and a homogeneous and high signal intensity on axial T2-weighted images (Fig. 3B) and is homogeneous enhanced on axial postcontrast T1-weighted image (Fig. 3C); 3D-ASL CBF map (Fig. 3D) shows relative hyperperfusion; HE staining (Fig. 3E) indicated meningioma.

突破鞍隔时冠状位可见典型“束腰征”，易囊性变、出血、坏死<sup>[12]</sup>。二者的鉴别点关键在于确定肿瘤主体部分的位置，本研究4例误诊病例中3例位于颈内动脉外侧，垂体均显示不清。海绵状血管瘤肿瘤主体多位于鞍外，冠状位更易于显示二者关系。误诊脑膜瘤的原因可能为，一方面脑膜瘤是颅内最常见的非胶质细胞肿瘤，鞍旁脑膜瘤约占除垂体瘤外鞍区肿瘤的15%，占所有脑膜瘤的20%-30%<sup>[13]</sup>，鞍旁海绵状血管瘤极易误诊为脑膜瘤，尤其是血管瘤型，二者发病年龄相似，均好发于中年女性。另一方面，二者的信号特点相似，MRI平扫T1WI均可以表现为低或等信号，T2WI表现为稍高于脑脊液的信号，5例误诊病例中3例T2WI表现为极高信号，增强扫描均可以表现为均匀

或不均匀强化<sup>[14]</sup>，另外二者均可以单独累及鞍旁或同时累及鞍内外，且都有可能有血管流空影像，可有或无脑膜尾征，误诊病例中2例出现脑膜尾征，误诊病例中2例出现脑膜尾征，其中一例病灶通过视神经管向肌锥内侵犯，此征象更易误诊为脑膜瘤。因此，信号特点及脑膜尾征不能作为血管型脑膜瘤的唯一诊断特征，同病异影，异病同征，二者的鉴别较为困难，需借助其它技术。

MRI除平扫及增强技术外，磁共振波谱(MRS)技术及弥散加权成像(DWI)能够辅助鉴别鞍旁海绵状血管瘤及脑膜瘤，脑膜瘤波谱可表现为胆碱峰增高，没有肌酸和N-乙酰天门冬氨酸峰；而海绵状血管瘤无明显肿瘤细胞增生，则表现为胆碱、肌

酸和 N-乙酰天门冬氨酸峰均消失,可有脂质峰<sup>[15]</sup>,海绵状血管瘤因其无明显肿瘤细胞,DWI 轻度弥散受限,表现为等或稍低信号,ADC 值稍高<sup>[16]</sup>;脑膜瘤因肿瘤细胞密集,细胞间隙小,限制了水分子的扩散,ADC 值仅仅稍高于脑白质<sup>[17]</sup>。但两种扫描技术存在缺陷,首先鞍旁容易受气体及周围骨质的影响,磁敏感伪影大,另外周围组织结构很难被饱和,扫描往往不理想。近年来,3D-ASL 临床应用广泛,避免了鞍区磁敏感伪影产生的干扰,该技术基于动脉血自旋标记技术,全脑无需注药反映病变灌注特征,肿瘤病变的对比剂增强扫描和灌注成像反映的是病变不同的病理改变,灌注成像能真正反映出肿瘤的新生血管<sup>[18]</sup>。陆续有研究表明该技术对于鞍旁脑膜瘤与鞍旁海绵状血管瘤的鉴别诊断具有重要临床价值,尤其是当 MRI 影像特点与临床表现相似,且难以明确时。

本研究有 5 例行 3D-ASL 检查,因 CBF 图均呈低灌注状态,避免误诊其为脑膜瘤。脑膜瘤虽然镜检因不同的病理亚型呈现不同的组织特点,都含有脑膜上皮细胞,瘤细胞间可见纤维组织、血管等间质,是颅脑最富于血供的肿瘤,由额外动脉分支供血,肿瘤血供丰富,因此 CBF 图呈高灌注状态<sup>[19]</sup>;而海绵状血管瘤缺乏真正的肿瘤供血动脉和成熟的引流静脉,CBF 图呈低灌注状态<sup>[20]</sup>。另有研究<sup>[21]</sup>表明脑膜瘤的 nCBF 值明显高于海绵状血管瘤,且病灶区 minADC 值与 3D-ASL 中定量参数 nCBF 呈负相关,二者相关性较好。由于病例较少,本研究采用 3D-ASL 技术未对该疾病进行定量研究,尚待进一步大量数据研究证实。

综上所述,鞍旁海绵状血管瘤同脑膜瘤和垂体瘤鉴别诊断较困难,除抓住 MRI 重要形态学特征外,对于与其它肿瘤较难鉴别者,3D-ASL 从功能学角度可作为有效补充手段,具有重要的临床应用前景。

#### 参考文献(References)

- [1] Tannouri F, Divano L, Caucheteur V, et al. Cavernous haemangioma in the cavernous sinus: case report and review of the literature [J]. Neuroradiology, 2001, 43(4): 317-320
- [2] Wang X, Mei G, Liu X, et al. The role of stereotactic radiosurgery in cavernous sinus hemangiomas: a systematic review and meta-analysis [J]. J Neurooncol, 2012, 107(2): 239-245
- [3] Chuang C C, Jung S M, Yang J T, et al. Intrasellar cavernous hemangioma[J]. J Clin Neurosci, 2006, 13(6): 672-675
- [4] Tang X, Wu H, Wang B, et al. A new classification and clinical results of Gamma Knife radiosurgery for cavernous sinus hemangiomas: a report of 53 cases[J]. Acta Neurochir (Wien), 2015, 157(6): 961-969, 969
- [5] Zhou L F, Mao Y, Chen L. Diagnosis and surgical treatment of cavernous sinus hemangiomas: an experience of 20 cases [J]. Surg Neurol, 2003, 60(1): 31-36, 36-37
- [6] Elster A D, Challa V R, Gilbert T H, et al. Meningiomas: MR and histopathologic features[J]. Radiology, 1989, 170(3 Pt 1): 857-862
- [7] 姚振威, 冯晓源. 海绵窦海绵状血管瘤的 MRI 特征[J]. 中国医学计算机成像杂志, 2010, (03): 185-188  
Yao Zhen-wei, Feng Xiao-yuan. MRI features of cavernous hemangioma in cavernous sinus [J]. Chinese Computed Medical Imaging, 2010, (03): 185-188
- [8] Jinhu Y, Jianping D, Xin L, et al. Dynamic enhancement features of cavernous sinus cavernous hemangiomas on conventional contrast-enhanced MR imaging[J]. AJNR Am J Neuroradiol, 2008, 29 (3): 577-581
- [9] 王凯, 张占普, 窦长武, 等. 鞍内海绵状血管瘤一例报道并文献复习 [J]. 中华临床医师杂志(电子版), 2014, (17): 3193-3196  
Wang Kai, Zhang Zhan-pu, Dou Chang-wu, et al. A case report and literature review of intrasellar cavernous hemangioma [J]. Chinese Journal of Clinicians(Electronic Edition), 2014, (17): 3193-3196
- [10] Tokunaga K, Date I. Clinical features and management of cavernous and venous angiomas in the head[J]. Brain Nerve, 2011, 63(1): 17-25
- [11] Tian Y M, Xiao L H, Gao X W. Adhesion of cavernous hemangioma in the orbit revealed by CT and MRI: analysis of 97 cases [J]. Int J Ophthalmol, 2011, 4(2): 195-198
- [12] 牛磊, 朱蒙蒙, 王明皓, 等. 鞍旁海绵状血管瘤的 MRI 诊断 [J]. 医学影像学杂志, 2013(07): 998-1000  
Niu Lei, Zhu Meng-meng, Wang Ming-hao, et al. MRI diagnosis of parasellar cavernous hemangioma [J]. Journal of Medical Imaging, 2013(07): 998-1000
- [13] Bladowska J, Zimny A, Guzinski M, et al. Usefulness of perfusion weighted magnetic resonance imaging with signal-intensity curves analysis in the differential diagnosis of sellar and parasellar tumors: preliminary report[J]. Eur J Radiol, 2013, 82(8): 1292-1298
- [14] Jinhu Y, Jianping D, Xin L, et al. Dynamic enhancement features of cavernous sinus cavernous hemangiomas on conventional contrast-enhanced MR imaging[J]. AJNR Am J Neuroradiol, 2008, 29 (3): 577-581
- [15] 鱼博浪, 王斐, 孙亲利, 等. 鞍旁海绵状血管瘤的 CT 和 MRI 诊断 [J]. 临床放射学杂志, 2007, (02): 117-119  
Yu Bo-lang, Wang Fei, Sun Qin-li, et al. The diagnosis of cavernous angioma in the cavernous sinus with CT and MRI [J]. Journal of Clinical Radiology, 2007, (02): 117-119
- [16] Nam S J, Park K Y, Yu J S, et al. Hepatic cavernous hemangiomas: relationship between speed of intratumoral enhancement during dynamic MRI and apparent diffusion coefficient on diffusion-weighted imaging[J]. Korean J Radiol, 2012, 13(6): 728-735
- [17] Bitzer M, Klose U, Geist-Barth B, et al. Alterations in diffusion and perfusion in the pathogenesis of peritumoral brain edema in meningiomas[J]. Eur Radiol, 2002, 12(8): 2062-2076
- [18] Hakyemez B, Erdogan C, Bolca N, et al. Evaluation of different cerebral mass lesions by perfusion-weighted MR imaging [J]. J Magn Reson Imaging, 2006, 24(4): 817-824
- [19] Ginat D T, Mangla R, Yeaney G, et al. Correlation between dynamic contrast-enhanced perfusion MRI relative cerebral blood volume and vascular endothelial growth factor expression in meningiomas [J]. Acad Radiol, 2012, 19(8): 986-990
- [20] Salanitri G C, Stuckey S L, Murphy M. Extracerebral cavernous hemangioma of the cavernous sinus: diagnosis with MR imaging and labeled red cell blood pool scintigraphy [J]. AJNR Am J Neuroradiol, 2004, 25(2): 280-284
- [21] Xiao H F, Lou X, Liu M Y, et al. The role of magnetic resonance diffusion-weighted imaging and three-dimensional arterial spin labelling perfusion imaging in the differentiation of parasellar meningioma and cavernous haemangioma[J]. J Int Med Res, 2014, 42 (4): 915-925